SpringerPlus
a SpringerOpen Journal

RESEARCH   **Open Access**

Mutant LV$^{476-7}$AA of A-subunit of *Enterococcus hirae* V$_1$-ATPase: High affinity of A$_3$B$_3$ complex to DF axis and low ATPase activity

Jahangir Alam[1,2*], Ichiro Yamato[1], Satoshi Arai[1,3], Shinya Saijo[1,4,5], Kenji Mizutani[1,3], Yoshiko Ishizuka-Katsura[6,7], Noboru Ohsawa[6,7], Takaho Terada[6,8], Mikako Shirouzu[6,7], Shigeyuki Yokoyama[6,8], So Iwata[6,7,9], Yoshimi Kakinuma[10] and Takeshi Murata[3,6,7,11]

Abstract

Vacuolar ATPase (V-ATPase) of *Enterococcus hirae* is composed of a soluble functional domain V$_1$ (A$_3$B$_3$DF) and an integral membrane domain V$_o$ (ac), where V$_1$ and V$_o$ domains are connected by a central stalk, composed of D-, F-, and d-subunits; and two peripheral stalks (E- and G-subunits). We identified 120 interacting residues of A$_3$B$_3$ heterohexamer with D-subunit in DF heterodimer in the crystal structures of A$_3$B$_3$ and A$_3$B$_3$DF. In our previous study, we reported 10 mutants of *E. hirae* V$_1$-ATPase, which showed lower binding affinities of DF with A$_3$B$_3$ complex leading to higher initial specific ATPase activities compared to the wild-type. In this study, we identified a mutation of A-subunit (LV$^{476-7}$AA) at its C-terminal domain resulting in the A$_3$B$_3$ complex with higher binding affinities for wild-type or mutant DF heterodimers and lower initial ATPase activities compared to the wild-type A$_3$B$_3$ complex, consistent with our previous proposal of reciprocal relationship between the ATPase activity and the protein-protein binding affinity of DF axis to the A$_3$B$_3$ catalytic domain of *E. hirae* V-ATPase. These observations suggest that the binding of DF axis at the contact region of A$_3$B$_3$ rotary ring is relevant to its rotation activity.

Keywords: Site-directed mutation; Reconstitution; Catalytic domain; ATPase assay; Surface plasmon resonance; *Enterococcus hirae*

Introduction

Vacuolar ATPase (V-ATPase) functions as a proton pump in the acidic organelles and plasma membranes of eukaryotic cells and bacteria (Forgac 2007; Stevens & Forgac 1997). This acidic environment is essential for such processes as receptor-mediated endocytosis, intracellular targeting of lysosomal enzymes, protein processing and degradation (Forgac 2007). ATPases possess an overall similar structure composed of a catalytic portion (F$_1$-, V$_1$-, or A$_1$-ATPase) and a membrane-embedded ion-transporting portion (F$_o$-, V$_o$-, or A$_o$-ATPase), and have a similar reaction mechanism as rotary motors (Forgac 2007).

V-ATPases are found in bacteria, such as *Thermus thermophilus* and *Enterococcus hirae*. *T. thermophilus* V-ATPase physiologically functions as an ATP synthase (Lee et al. 2010), whereas, *E. hirae* V-ATPase is not an ATP synthase and instead acts as a primary ion pump similar to eukaryotic V-ATPases, which transports Na$^+$ or Li$^+$ instead of H$^+$ (Murata et al. 2000, Murata et al. 2005b, 2008; Furutani et al. 2011; Mizutani et al. 2011). The enzyme is composed of nine subunits having amino acid sequences that are homologous to those of the corresponding subunits of eukaryotic V-ATPases (Murata et al. 1997, 2005a; Yamamoto et al. 2008; Zhou et al. 2011). Amino acid sequences and subunit structures are more similar to eukaryotic V-ATPases than to ATP synthases of F- and V-ATPases. The V$_1$ domain of V-ATPase is composed of a hexameric arrangement of alternating A- and B-subunits responsible for ATP binding and hydrolysis (Murata et al. 1999) and the V$_o$ domain is composed of the 16-kDa c-subunits and an a-subunit

* Correspondence: jalambioru@yahoo.com
[1]Department of Biological Science and Technology, Tokyo University of Science, 6-3-1 Niijuku, Katsushika-ku, Tokyo 125-8585, Japan
[2]Department of Genetic Engineering and Biotechnology, School of Life Sciences, Shahjalal University of Science and Technology, Sylhet 3114, Bangladesh
Full list of author information is available at the end of the article

Springer

in which rotational energy is converted to drive Na^+ translocation (Furutani et al. 2011; Mizutani et al. 2011). The V_1 and V_o domains are connected by a central stalk (composed of D-, F-, and d-subunits) and 2 peripheral stalks (composed of E- and G-subunits of V_1) (Murata et al. 2005a & Yamamoto et al. 2008). During ATP hydrolysis, the central axis (the DFd complex) attached on the membrane c-ring rotates inside the hexagonally arranged A_3B_3 complex, which causes ion pumping at the interface between the c-ring and a-subunit (Murata et al. 2008). Single molecular studies of *E. hirae* V_1-ATPase showed 120° steps of rotation without any substeps driven by ATP hydrolysis, as commonly seen with F_1-ATPase (Minagawa et al. 2013). Previously, we reported the reconstitution and purification of A_3B_3 and A_3B_3DF of *E. hirae* V-ATPase (Arai et al. 2009) and solved the crystal structures of DF, A_3B_3, and A_3B_3DF (Arai et al. 2013; Saijo et al. 2011). Crystal structures of these complexes suggest the existence of 120 polar and nonpolar (van der Waals) interactions between the A_3B_3 and DF complexes and ATP hydrolysis seems to be stimulated by the approach of a conserved arginine residue (Arai et al. 2013). Recently, we reported the mutational effects of 10 interacting residues at the conserved C-terminal domain (near the $^{480}DSLSDND^{486}$ sequence of A-subunit (Figure 1F), probably corresponding to the DELSEED sequence of F-ATPase (Mnatsakanyan et al. 2011; Nakanishi-Matsui & Futai 2008)) of A- and B-subunits with the residues of D-subunit, showing higher initial ATPase activities and lower binding affinities compared to the wild-type (Alam et al. 2013).

In this study, we constructed another mutant ($LV^{476-7}AA$) (Figure 1B) neighboring to the $^{480}DSLSDND^{486}$ sequence (Figure 1F) of A-subunit. We reconstituted the V_1 domains containing different mutational combinations including wild-type and previous mutations (Alam et al. 2013) (Figure 1C-E) and measured the initial ATPase activities and binding affinities of those V_1-ATPases that showed higher binding affinities and lower initial ATPase activities than that of the wild-type.

Results

Reconstitution and purification of $A(LV^{476-7}AA)_3B_3$ and $A(LV^{476-7}AA)_3B(L^{389}A)_3$ heterohexamers

From the crystal structures of A_3B_3 and A_3B_3DF (Arai et al. 2013), we identified LV^{476-7} of A-subunit and L^{389} of B-subunit located closely with the interacting D-subunit in the "tight" form (A_{CR}-B_{CR} pair) of V_1-ATPase (Figure 1C). So, in this study we used the previously constructed $L^{389}A$ mutant of B-subunit (Alam et al. 2013) to reconstitute $A(LV^{476-7}AA)_3B(L^{389}A)_3$ heterohexamer. $A(LV^{476-7}AA)$ monomer showed a very low efficiency of complex formation with either wild-type B or B ($L^{389}A$) monomer in the presence of 2 mM ATP, distinct from wild-type (Arai et al. 2009), but we found that $A(LV^{476-7}AA)$ showed efficient reconstitution of $A(LV^{476-7}AA)_3B_3$ and $A(LV^{476-7}AA)_3B(L^{389}A)_3$ heterohexamers in the presence of 200 μM AMP-PNP (analogue
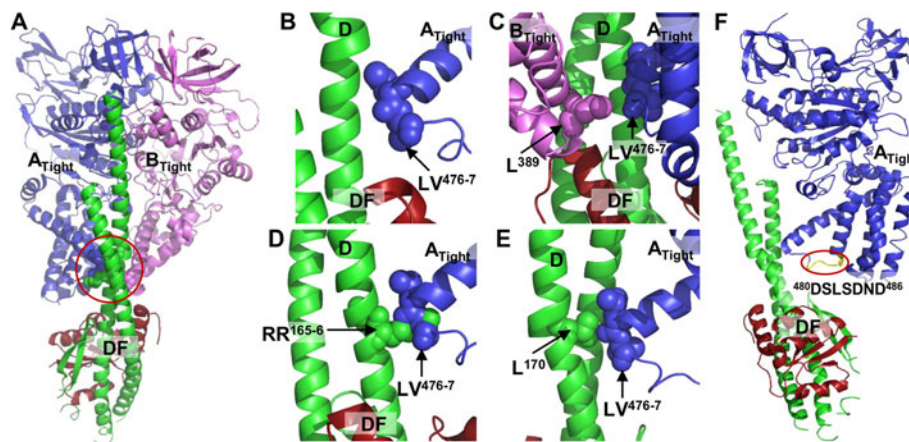

Figure 1 Positions of the critical contact residues of A- and/or B-subunits with DF complex in the structure of *E. hirae* V_1-ATPase (Arai et al. 2013; Saijo et al. 2011). (A) The side-viewed ribbon representation of the "tight" form of A- (*tv_blue*) and B-subunit (*violet*) together with DF (*tv_green* and *firebrick*, respectively) complex. Spheres (in *red circle*) indicate the selected residues (Figure 1B-E) for mutation of the corresponding subunits. **(B)** The closer view of the critical contact residue LV^{476-7} (*tv_blue spheres*) of the A-subunit with DF complex. **(C)** The closer view of the critical contact residues (LV^{476-7} (*tv_blue spheres*) of A-subunit and L^{389} (*violet spheres*) of B-subunit) of the "tight" form of A- and B-subunits together with DF complex. **(D)** The closer view of the "tight" form of A-subunit together with DF complex showing the critical contact residues; LV^{476-7} (*tv_blue spheres*) of A-subunit and RR^{165-6} (*tv_green spheres*) of D-subunit. **(E)** The closer view of the "tight" form of A-subunit together with DF complex showing the critical contact residues; LV^{476-7} (*tv_blue spheres*) of A-subunit and L^{170} (*tv_green spheres*) of D-subunit. **(F)** The "tight" form of A-subunit (*tv_blue*) together with DF (*tv_green* and *firebrick*, respectively) complex showing the $^{480}DSLSDND^{486}$ sequence of A-subunit (*yellow* in *red circle*), probably corresponding to the DELSEED sequence of F-ATPase (Mnatsakanyan et al. 2011; Nakanishi-Matsui & Futai 2008).

of ATP) instead of 2 mM ATP (Figure 2A, *lane 1*). Both mutant heterohexamers were purified by gel-filtration chromatography (Figure 2A-B). These complexes seemed stable in the absence of nucleotides, although $A(LV^{476-7}AA)_3B_3$ and $A(LV^{476-7}AA)_3B(L^{389}A)_3$ heterohexamers showed lower stability than the wild-type A_3B_3; in native PAGE, a band at position of $A(LV^{476-7}AA)_1B_1$ or $A(LV^{476-7}AA)_1B(L^{389}A)_1$ complex was observed after a few days storage at $-80°C$ and $A(LV^{476-7}AA)_3B(L^{389}A)_3$ heterohexamer dissociated into monomers after a few weeks storage at 4°C (Figure 2A, *lane 4* (after 2–3 weeks stored at 4°C)).

Reconstitution of A_3B_3DF (V_1 domain) complex

$A(LV^{476-7}AA)_3B_3$ and $A(LV^{476-7}AA)_3B(L^{389}A)_3$ hetero-hexamers formed V_1 domains ($A(LV^{476-7}AA)_3B_3DF$ and $A(LV^{476-7}AA)_3B(L^{389}A)_3DF$ complex, respectively) of V-ATPase with DF heterodimer (Figure 2A). When $A(LV^{476-7}AA)_3B_3$ and $A(LV^{476-7}AA)_3B(L^{389}A)_3$ heterohexamers were incubated with DF heterodimer in the absence of nucleotides, both heterohexamers formed catalytic domains, $A(LV^{476-7}AA)_3B_3DF$ and $A(LV^{476-7}AA)_3B(L^{389}A)_3DF$, respectively (Figure 2A), showing the similar extent of reconstitution of V_1 domains as the wild-type. The crystal structures of A_3B_3 and A_3B_3DF (Arai et al. 2013) suggested that LV^{476-7} of A-subunit closely reside to the RR^{165-6} and L^{170} of D-subunit when V_1 is in its "tight" form (Figure 1D-E). So, we reconstituted two additional mutant V_1 domains; $A(LV^{476-7}AA)_3B_3D(RR^{165-6}AA)F$ and $A(LV^{476-7}AA)_3B_3D(L^{170}N)F$, showing

the similar reconstitution efficiencies in native-PAGE like as the wild-type (data not shown), which indicates similar structural integrity of the purified mutant V_1-ATPases.

Biochemical properties of the reconstituted mutant catalytic domains

Initial specific activities of the reconstituted $A(LV^{476-7}AA)_3B_3DF$ and $A(LV^{476-7}AA)_3B(L^{389}A)_3DF$ complexes (7.9 units/mg and 9.1 units/mg, respectively, Figure 3A, Table 1) were about half of the wild-type (16.0 units/mg). The K_m values for ATP of $A(LV^{476-7}AA)_3B_3DF$ and $A(LV^{476-7}AA)_3B(L^{389}A)_3DF$ complexes were not so much different (0.45 mM and 0.27 mM, respectively) from that of wild-type ($K_m = 0.4$ mM) (Figure 3B) and reconstituted $A(LV^{476-7}AA)_3B_3D(RR^{165-6}AA)F$ and $A(LV^{476-7}AA)_3B_3D(L^{170}N)F$ complexes showed almost similar initial specific activities (15.5 units/mg and 13.0 units/mg, respectively, Table 1) like as the wild-type (16.0 units/mg).

$A(LV^{476-7}AA)_3B_3$ heterohexamer showed higher binding affinity (dissociation constant, K_D 1.1 nM, Table 1) to wild-type DF heterodimer than the wild-type A_3B_3 complex (K_D 1.6 nM, Table 1) and other mutational combinations of A_3B_3 and DF complexes showed binding affinities between these ranges (Table 1). These findings (Table 1) indicate that lower ATPase activity (probably the rotation speed) is due to the tight binding of the DF axis to the rotary ring A_3B_3. There was one exception to this rule; the mutant $A(LV^{476-7}AA)_3B_3$ heterohexamer showed
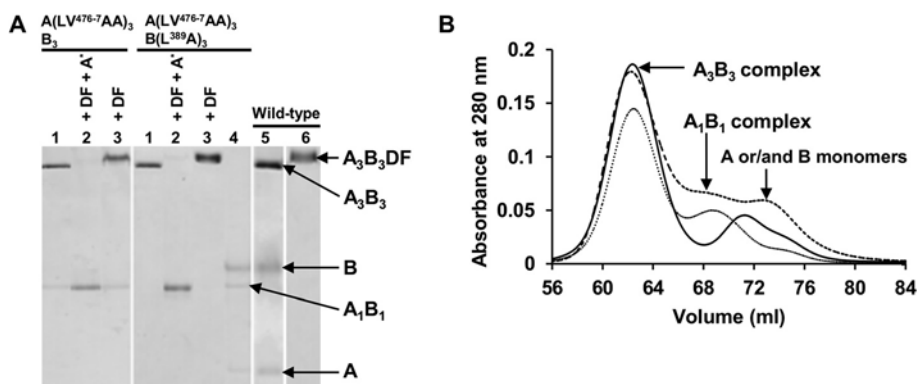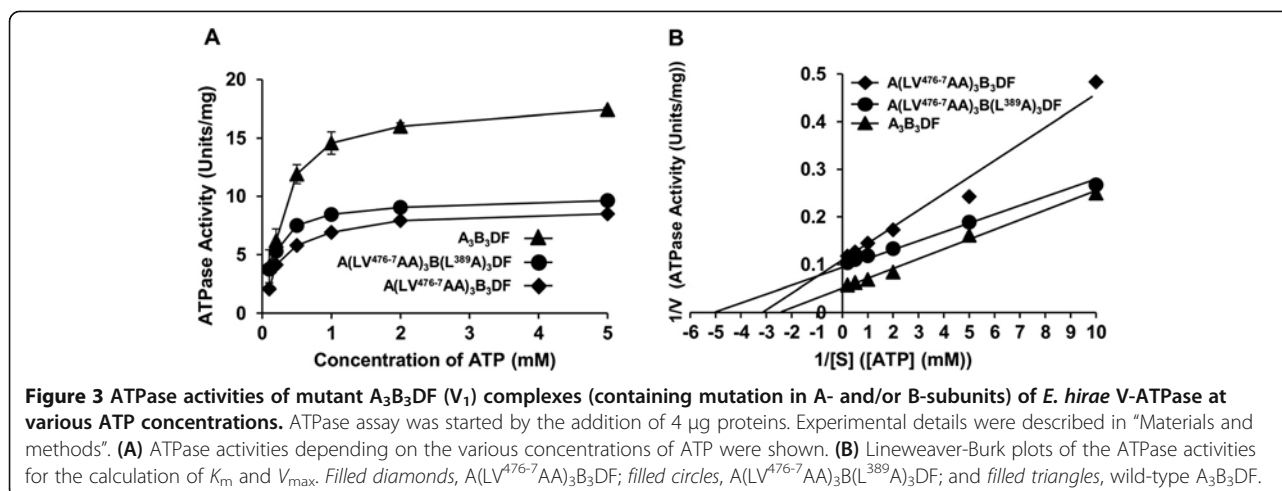

Figure 2 Basic native-PAGE pattern and gel-filtration profiles for the reconstitution and purification of A_3B_3 complexes from A- and B-monomers. (A) Basic native-PAGE pattern stained with CBB R-250. *Lane 1*, gel-filtration purified mutant A_3B_3 heterohexamers reconstituted with 200 μM AMP-PNP; *lane 2*, reconstituted mutant A_3B_3 heterohexamers with DF heterodimer in the presence of 2 mM AMP-PNP; *lane 3*, reconstituted mutant A_3B_3 heterohexamers with DF heterodimer without nucleotides; *lane 4*, purified $A(LV^{476-7}AA)_3B(L^{389}A)_3$ heterohexamer after storage at 4 °C for 20 days; *lane 5*, wild-type A_3B_3 with A and B monomers; and *lane 6*, wild-type A_3B_3DF. One μg of protein was loaded in each lane. A* indicates addition of AMP-PNP. **(B)** Gel-filtration profiles for the purification of mutant A_3B_3 heterohexamers reconstituted from A and B monomers. *Dotted line*, $A(LV^{476-7}AA)_3B_3$; *dashed line*, $A(LV^{476-7}AA)_3B(L^{389}A)_3$; and *solid line*, wild-type A_3B_3. Gel-filtration was performed as described in "Materials and methods". Mixture of total 6.1 mg (mixing ratio of A- and B-subunits were A:B = 65:52 (1:1 molar ratio)) samples in buffer A were loaded in Superose 6 pg gel-filtration column (500 × 16 mm ID) (GE Healthcare) and eluted with the same buffer. Purified A_3B_3 complex by gel-filtration was examined on basic native-PAGE as lane 1 (as shown in Figure 2A).

Figure 3 ATPase activities of mutant A_3B_3DF (V_1) complexes (containing mutation in A- and/or B-subunits) of *E. hirae* V-ATPase at various ATP concentrations. ATPase assay was started by the addition of 4 μg proteins. Experimental details were described in "Materials and methods". **(A)** ATPase activities depending on the various concentrations of ATP were shown. **(B)** Lineweaver-Burk plots of the ATPase activities for the calculation of K_m and V_{max}. *Filled diamonds*, $A(LV^{476-7}AA)_3B_3DF$; *filled circles*, $A(LV^{476-7}AA)_3B(L^{389}A)_3DF$; and *filled triangles*, wild-type A_3B_3DF.

very low binding affinity for $D(RR^{165-6}AA)F$ (Table 1) with similar initial specific activity like as the wild-type.

Discussion

In this study, we selected the amino acid residues for mutation at the contact regions of C-terminal domain of the A-subunit (Figure 1B-E) (Arai et al. 2013). During ATP hydrolysis by V_1-ATPase, D-subunit rotates inside the hexagonally arranged A_3B_3 complex and comes in contact to the residues of A- and/or B-subunits, which probably correspond to the conserved DELSEED-loop of the β-subunit of F-ATPase (Mnatsakanyan et al. 2011; Nakanishi-Matsui & Futai 2008). From structure and sequence analysis of *E. hirae* V-ATPase, we considered the residues $^{480}DSLSDND^{486}$ of A-subunit (Figure 1F) is the corresponding loop of DELSEED of F-ATPase. We substituted the amino acids leucine and valine with alanine because of its stable helix forming tendency (Rohl et al. 1999). We demonstrated that purified mutant monomers- $A(LV^{476-7}AA)$ and $B(L^{389}A)$ were capable to form heterohexamers, $A(LV^{476-7}AA)_3B_3$ and $A(LV^{476-7}AA)_3B(L^{389}A)_3$, like as the wild-type (Figure 2A) (Arai et al.

2009). They formed catalytic domains (V_1-ATPases) with wild-type/mutant DF heterodimers as the similar extent of the wild-type. These mutant V_1-ATPases were functionally active and showed different initial specific activities depending on the nature of the amino acid substituted. Hydrophilic/polar arginine (Arakawa et al. 2007) or strong hydrophobic/non-polar amino acids like as valine or leucine may form stronger interaction with other polar or non-polar amino acids, respectively, in proteins. From the crystal structures of *E. hirae* V_1-ATPase (Arai et al. 2013; Saijo et al. 2011), we found that C-terminal residues of A-subunit, LV^{476-7} (of A_{CR}-B_{CR} pair in "tight" form) are in close contact with R^{165}, L^{170} (Figure 1D-E) and some other residues of D-subunit. Also, a residue at the corresponding region of B-subunit-L^{389} (of A_{CR}-B_{CR} pair) is closely located near LV^{476-7} residues of A-subunit (Figure 1C). We expected that these closely residing amino acids should have strong interactions with each other which should be influential to the rotation activity. So, we selected those neighboring residues of $^{480}DSLSDND^{486}$ sequence of A-subunit (Figure 1F) and changed all these arginine, leucine, and valine to

Table 1 Summary of ATPase activities of V_1 complexes containing mutant A_3B_3 heterohexamers and wild-type/mutant DF heterodimers and the binding affinities of those mutants measured by SPR assay

Protein	Initial specific activity (units/mg)[*]	K_D (nM) (using mutant A_3B_3 as ligand and mutant/wild-type DF as analyte)
$A(LV^{476-7}AA)_3B_3DF$	7.9 ± 0.3	1.1 ± 0.2
$A(LV^{476-7}AA)_3B(L^{389}A)_3DF$	9.1 ± 0.2	1.2 ± 0.1
$A(LV^{476-7}AA)_3B_3D(RR^{165-6}AA)F$	15.5 ± 1.4	50.9 ± 8.4
$A(LV^{476-7}AA)_3B_3D(L^{170}N)F$	13.0 ± 0.3	1.4 ± 0.3
Wild-type A_3B_3DF	16.0 ± 0.2	1.6 ± 0.1

ATPase activities of the reconstituted mutant A_3B_3DF's were measured using ATP regenerating system (Alam et al. 2013 & Murata et al. 2001). ATPase assay was started by the addition of 4 μg proteins. For SPR assays, different concentrations of analyte wild-type/mutant DF heterodimer were injected onto the sensor chip Ni-NTA surface having immobilized mutant A_3B_3 heterohexamers. Reconstituted mutant A_3B_3 heterohexamers and wild-type/mutant DF heterodimer were diluted in running buffer (20 mM MES-Tris, pH 6.5; 150 mM NaCl; 50 μM EDTA-Na; 0.005% polyoxyethylene (20) sorbitol monolaurate). Experimental details were described in "Materials and methods".
[*]"Initial specific activity" was calculated by measuring the specific activity during the first minute of the assay (starting from the 16th second) after adding proteins.

relatively low hydrophobic and helix forming alanine. We assumed that by substitution with alanine, the binding affinities should decrease leading to higher ATPase activities. But unexpectedly all the mutant A_3B_3DFs containing $A(LV^{476-7}AA)$ mutation showed similar to lower initial specific activities with higher binding affinities than those of the wild-type (Figure 3A, Table 1). From this observation, we speculated that the substitution of two larger amino acids (leucine and valine) by smaller amino acid (alanine) may have resulted in a slight conformational difference of A-subunit which might be suitable for closer contact with D-subunit. Substitution effects of all the DELSEED loop residues with alanine have been already reported to resulting in the similar unidirectional rotation with kinetic parameters comparable to those of the wild-type F_1 (Tanigawara et al. 2012). Substitution of each residue and all five acidic residues in the DELSEED sequence with alanine resulted in the similar torque as the wild-type (Hara et al. 2000). Moreover, recently Usukura et al. (Usukura et al. 2012) reported that deletion of one or two turns in the α-helix at the DELSEED region in the C-terminal domain of catalytic β subunit at the rotor/central stalk contact region of *Bacillus* PS3 F_1-ATPase reduced the torque as well as ATPase activity to about half of the wild-type. Their result indicated that the mutants with the shortened loop can synthesize ATP and produce normal torque (Usukura et al. 2012) and ATPase activity. It would be interesting if we obtain 3D structures of these mutant A_3B_3DF or $α_3β_3γ$ to see the structural difference from wild-type and to estimate the interaction strength with DF or γ subunit. Considering their report (Usukura et al. 2012), we have tried to obtain several deletion mutants of A-subunit at the contact site with D-subunit, but they could not be purified, probably due to their instability. When we replaced leucine (L) to asparagine (N) (in case of D mutant, $D(L^{170}N)$), we found almost similar ATPase activity as the wild-type and small difference of binding affinity correlating with initial specific activities (Table 1).

In our previous study, we observed relationship of higher ATPase activity with lower binding affinity of $D(RR^{165-6}$ AA) mutant with wild-type A_3B_3 complex (Alam et al. 2013). When this mutant formed V_1 complex with $A(LV^{476-7}AA)_3B_3$, it showed very low binding affinity with high ATPase activity (compared to $A(LV^{476-7}AA)_3B_3DF$, Table 1), not higher than the wild-type A_3B_3DF; this low ATPase activity may be because of the dissociation of some DF heterodimer during ATPase assay owing to the low affinity, consistent with the expectation that RR^{165-6} of D-subunit is closely located to LV^{476-7} of A-subunit in "tight" form (A_{CR}-B_{CR} pair) of our crystal structures (Figure 1D) (Arai et al. 2013; Saijo et al. 2011). V_1-ATPase combined with A ($LV^{476-7}AA$) and $D(L^{170}N)F$ mutants gave compensating

effect showing nearly similar specific activities and binding affinities to those of each single mutant, suggesting the substantial interaction between $A(LV^{476-7})$ and $D(L^{170})$ (Table 1), consistent with our crystal structures (Figure 1E) (Arai et al. 2013; Saijo et al. 2011).

Materials and methods
Expression and purification of wild-type/mutant A- and B-subunits, and DF subcomplex
Synthesized DNA fragments corresponding to the *A* and *B* genes with optimal codon usage for an *Escherichia coli* expression system were cloned into the plasmid vector pET23d (Arai et al. 2009). Mutant A-subunit was constructed using the wild-type *A* gene in the plasmid as the template for PCR-generated mutation. Wild-type/ mutant A- and B-subunits were independently expressed in *E. coli* BL21 (DE3) in modified-Davis Mingioli-Casamino Acid (m-DM-CA) medium (Mogi & Anraku, 1984) at 30°C as described in a previous report (Arai et al. 2009). Proteins were purified essentially according to the reported method (Arai et al. 2009; Alam et al. 2013) using Ni-Sepharose 6 fast flow (GE Healthcare) and gel-filtration chromatography (Superose 6 pg column (500 × 16 mm ID) (GE Healthcare)). Purified proteins were analyzed by sodium dodecyl sulfate-polyacrylamide gel electrophoresis (SDS-PAGE) and subsequently stained with CBB R-250. Purified proteins were concentrated by ultrafiltration using Amicon Ultra-4 30 K filters (Millipore Corporation, USA) and stored at −80°C until use. From 1 liter culture, the amount of purified $A(LV^{476-7}AA)$ proteins obtained was 20 mg. We also tried to obtain a deletion mutant $ΔRLV^{475-7}$ of A-subunit at the C-terminal domain and also a double mutant $VL^{388-9}AA$ of B-subunit locating at the conserved region of D-subunit, but $VL^{388-9}AA$ could not be expressed and $ΔRLV^{475-7}$ was not purified due to its instability.

To synthesize the wild-type/mutant DF complex, an *E. coli* cell-free protein expression system was used, as described elsewhere (Kigawa et al. 2004), by using plasmids coding genes for D- and F-subunits. The expressed protein was purified as previously described (Yamamoto et al. 2008). Mutagenesis of D-subunit was performed using the QuikChange site-directed mutagenesis kit (Agilent Technologies) as described (Arai et al. 2013).

Reconstitution of mutant catalytic domains (A_3B_3DF/V_1) from reconstituted wild-type/mutant A_3B_3 heterohexamers and synthesized DF heterodimers
The A_3B_3 complex was reconstituted from the purified A- and B-subunits with slight modification of previous method (Arai et al. 2009; Alam et al. 2013) using 200 μM AMP-PNP instead of 2 mM ATP. Briefly, the purified A- and B-subunits (3.4 and 2.7 mg of A- and B-subunits, respectively, at a 1:1 molar ratio) were

mixed and the volume was adjusted to 4 mL with buffer A (20 mM MES-Tris, pH 6.5; 50 mM KCl; 10% glycerol; 5 mM $MgSO_4$; 0.1 mM DTT). The protein mixture was then incubated on ice for 1 h in the presence of 200 μM AMP-PNP and afterward concentrated to 100 μL by ultrafiltration using Amicon Ultra-4 30 K filters (Millipore Corporation, USA). Then, 4 mL of buffer A with AMP-PNP was added to dilute the protein solution, and the solution was concentrated again to 100 μL. This dilution/concentration process was repeated thrice without adding AMP-PNP. The A_3B_3 heterohexamer was finally purified using a Superose 6 pg column (500 × 16 mm ID) (GE Healthcare). Complex formation was confirmed by using basic native-PAGE as previously described (Alam et al. 2013). For the reconstitution of wild-type and mutant catalytic V_1 domain (A_3B_3DF), purified wild-type/mutant A_3B_3 heterohexamers and synthesized DF heterodimer were incubated on ice for 1 hour mixing at a 1:5 molar ratio (Arai et al. 2009; Alam et al. 2013) and the formation of the complexes were checked by using basic native-PAGE (Arai et al. 2009; Alam et al. 2013).

ATPase assay of the reconstituted mutant A_3B_3DF complexes

Initial ATPase activities of the reconstituted A_3B_3DF were measured by ATP regenerating system (Alam et al. 2013; Murata et al. 2001). The assay mixture contained various concentrations of ATP, 2.5 mM phosphoenolpyruvate, 50 μg/mL pyruvate kinase, 50 μg/mL lactate dehydrogenase, and 0.2 mM β-NADH (dipotassium salt) in 1 mL of assay buffer (25 mM MES-Tris (pH 6.5), 4 mM $MgSO_4$, 10% glycerol). The reaction was initiated by adding 4 μg proteins. The rate of ATP hydrolysis was monitored at 25°C in terms of the rate of oxidation of NADH, as determined by the decrease in absorbance at 340 nm. Specific activities were calculated as units/mg proteins, with 1 unit of ATPase activity being defined as hydrolysis of 1 μmol ATP/min. Initial ATPase activity was calculated by measuring the specific activity during the first minute (starting from the 16th second) after adding the proteins. The measurement was repeated three times and averaged and the standard deviation was calculated. K_m and V_{max} were calculated by fitting the averaged values as straight lines in Lineweaver-Burk plots.

Measurement of real-time binding affinity using surface plasmon resonance (SPR)

The binding affinity of DF complex to the reconstituted A_3B_3 complex was measured by SPR analysis on a Biacore T100 instrument (GE Healthcare Bio-sciences, AB, Sweden) as described previously (Alam et al. 2013; Arai et al. 2013; Saijo et al. 2011). The Biacore Ni-NTA sensor chip (GE Healthcare Bio-sciences) was activated with 0.5 μM $NiCl_2$ as described by the manufacturer. The reconstituted A_3B_3 complex was immobilized at a concentration of 35 μg/mL in running buffer (20 mM MES-Tris, pH 6.5; 150 mM NaCl; 50 μM EDTA-Na; 0.005% polyoxyethylene (20) sorbitol monolaurate), passing through the Biacore flow cell at a rate of 10 μL/min. A flow cell containing no protein served as a negative control. Different concentrations of DF complex were prepared as analyte in the running buffer. The obtained sensorgrams were evaluated using Biacore T100 evaluation software. The equilibrium constant for dissociation, K_D, were obtained using the Langmuir binding model (1:1 binding model).

Chemicals/reagents and other experimental protocols

Protein concentration was determined by DC Protein Assay Kit (Bio-Rad Laboratories) using bovine serum albumin as the standard. To check the purified proteins, SDS-PAGE was performed according to Laemmli (Laemmli 1970), and stained with Coomassie brilliant blue (CBB) R-250. Restriction enzymes were purchased from Nippon Gene Japan, New England BioLabs Japan, and Wako Pure Chem. Indust., Ltd. All other chemicals were of analytical grade and purchased from Sigma-Aldrich Japan KK or Wako Pure Chem. Indust., Ltd.

Abbreviations
CBB: Coomassie brilliant blue; DTT: Dithiothreitol; EDTA: Ethylenediamine-N,N, N′,N′-tetraacetic acid; IPTG: Isopropyl thio-β-galactoside; K_D: Dissociation constant; MES: 2-(N-morpholino) ethanesulphonic acid; m-DM-CA: Modified-Davis Mingioli-Casamino acid; SPR: Surface plasmon resonance; TEV: Tobacco etch virus; V-ATPase: Vacuolar ATPase.

Competing interest
The authors declare that they have no competing interest.

Authors' contributions
Conceived and designed the experiments: IY TM. Constructed A- and B-subunit mutants and performed experiments: MJA. Synthesized D-subunit mutants: KM YIK NO TT MS. Analyzed the data: MJA SA SS IY TM. Contributed reagents/materials/analysis tools: SY SI YK IY TM. Wrote the paper: MJA IY TM. All authors read and approved the final manuscript.

Author details
[1]Department of Biological Science and Technology, Tokyo University of Science, 6-3-1 Niijuku, Katsushika-ku, Tokyo 125-8585, Japan. [2]Department of Genetic Engineering and Biotechnology, School of Life Sciences, Shahjalal University of Science and Technology, Sylhet 3114, Bangladesh. [3]Department of Chemistry, Graduate School of Science, Chiba University, 1-33 Yayoi-choInage, Chiba 263-8522, Japan. [4]RIKEN SPring-8 Center, 1-1-1 Kouto, Sayo, Hyogo 679-5148, Japan. [5]Structural Biology Research Center, Photon Factory, Institute of Materials Structure Science, High Energy Accelerator Research Organization (KEK), Tsukuba, Ibaraki 305-0801, Japan. [6]RIKEN Systems and Structural Biology Center, 1-7-22 Suehiro-cho, Tsurumi, Yokohama 230-0045, Japan. [7]Division of Structural and Synthetic Biology, RIKEN Center for Life Science Technologies, 1-7-22 Suehiro-cho, Tsurumi, Yokohama 230-0045, Japan. [8]RIKEN Structural Biology Laboratory, 1-7-22 Suehiro-cho, Tsurumi, Yokohama 230-0045, Japan. [9]Department of Cell Biology, Faculty of Medicine, Kyoto University, Yoshidakonoe-cho, Sakyo-ku, Kyoto 606-8501, Japan. [10]Laboratory of Molecular Physiology

and Genetics, Faculty of Agriculture, Ehime University, 3-5-7 Tarumi, Matsuyama, Ehime 790-8566, Japan. [11]JST, PRESTO, 1-33 Yayoi-cho, Inage, Chiba 263-8522, Japan.

References

Alam MJ, Arai S, Saijo S, Suzuki K, Mizutani K, Ishizuka-Katsura Y, et al. (2013) Loose binding of the DF axis with the A_3B_3 complex stimulates the initial activity of *Enterococcus hirae* V_1-ATPase. PLoS One 8(9):1–9. doi:10.1371/journal.pone.0074291

Arai S, Yamato I, Shiokawa A, Saijo S, Kakinuma Y, Katsura YI, et al. (2009) Reconstitution *in vitro* of the catalytic portion (NtpA$_3$-B$_3$-D-G complex) of *Enterococcus hirae* V-type Na$^+$-ATPase. Biochem Biophys Res Commun 390:698–702

Arai S, Saijo S, Suzuki K, Mizutani K, Kakinuma Y, Ishizuka-Katsura Y, et al. (2013) Rotation mechanism of *Enterococcus hirae* V_1-ATPase based on asymmetric crystal structures. Nature 493:703–707

Arakawa T, Tsumoto K, Nagase K, Ejima D (2007) The effects of arginine on protein binding and elution in hydrophobic interaction and ion-exchange chromatography. Protein Expr Purif 54:110–116

Forgac M (2007) Vacuolar ATPases: Rotary proton pumps in physiology and pathophysiology. Nat Struct Mol Biol 8:917–929

Furutani Y, Murata T, Kandori H (2011) Sodium or lithium ion-binding-induced structural changes in the K-ring of V-ATPase from *Enterococcus hirae* revealed by ATR-FTIR spectroscopy. J Am Chem Soc 133:2860–2863

Hara KY, Noji H, Bald D, Yasuda R, Kinosita K, Jr, Yoshida M (2000) The role of the DELSEED motif of the b subunit in rotation of F_1-ATPase. J Biol Chem 275(19):14260–14263

Kigawa T, Yabuki T, Matsuda N, Matsuda T, Nakajima R, Tanaka A, et al. (2004) Preparation of *Escherichia coli* cell extract for highly productive cell-free protein expression. J Struct Funct Genomics 5:63–68

Laemmli UK (1970) Cleavage of structural proteins during the assembly of the head of bacteriophage T4. Nature 227:680–685

Lee LK, Stewart AG, Donohoe M, Bernal RA, Stock D (2010) The structure of the peripheral stalk of *Thermus thermophilus* H$^+$-ATPase/synthase. Nat Struct Mol Biol 17:373–378

Minagawa Y, Ueno H, Hara M, Ishizuka-Katsura Y, Ohsawa N, Terada T, et al. (2013) Basic properties of rotary dynamics of the molecular motor *Enterococcus hirae* V_1-ATPase. J Biol Chem 288(45):32700–32707

Mizutani K, Yamamoto M, Suzuki K, Yamato I, Kakinuma Y, Shirouzu M, et al. (2011) Structure of the rotor ring modified with N, N-dicyclohexylcarbodiimide of the Na + -transporting vacuolar ATPase. Proc Natl Acad Sci U S A 108:13474–13479

Mnatsakanyan N, Kemboi SK, Salas J, Weber J (2011) The β subunit loop that couples catalysis and rotation in ATP synthase has a critical length. J Biol Chem 286:29788–29796

Mogi T, Anraku Y (1984) Mechanism of proline transport in *Escherichia coli* K12. II. Effect of alkaline cations on binding of proline to a H$^+$/proline symport carrier in cytoplasmic membrane vesicles. J Biol Chem 259:7797–7801

Murata T, Takase K, Yamato I, Igarashi K, Kakinuma Y (1997) Purification and reconstitution of Na$^+$-translocating vacuolar ATPase from *Enterococcus hirae*. J Biol Chem 272:24885–24890

Murata T, Takase K, Yamato I, Igarashi K, Kakinuma Y (1999) Properties of the V_oV_1 Na$^+$-ATPase from *Enterococcus hirae* and its V_o moiety. J Biochem 125:414–421

Murata T, Igarashi K, Kakinuma Y, Yamato I (2000) Na$^+$ binding of V-type Na$^+$-ATPase in *Enterococcus hirae*. J Biol Chem 275:13415–13419

Murata T, Kakinuma Y, Yamato I (2001) ATP-dependent affinity change of Na$^+$-binding sites of V-ATPase. J Biol Chem 276:48337–48340

Murata T, Yamato I, Kakinuma Y (2005a) Structure and mechanism of vacuolar Na$^+$-translocating ATPase from *Enterococcus hirae*. J Bioenerg Biomembr 37:411–413

Murata T, Yamato I, Kakinuma Y, Leslie AGW, Walker JE (2005b) Structure of the rotor of the V-Type Na$^+$-ATPase from *Enterococcus hirae*. Science 308:654–659

Murata T, Yamato I, Kakinuma Y, Shirouzu M, Walker JE, Yokoyama S, et al. (2008) Ion binding and selectivity of the rotor ring of the Na$^+$-transporting V-ATPase. Proc Natl Acad Sci U S A 105:8607–8612

Nakanishi-Matsui M, Futai M (2008) Stochastic rotational catalysis of proton pumping F-ATPase. Philos Trans R Soc Lond B Biol Sci 363:2135–2142

Rohl CA, Fiori W, Baldwin RL (1999) Alanine is helix-stabilizing in both template-nucleated and standard peptide helices. Proc Natl Acad Sci U S A 96:3682–3687

Saijo S, Arai S, Hossain KMM, Yamato I, Suzuki K, Kakinuma Y, et al. (2011) Crystal structure of the central axis DF complex of the prokaryotic V-ATPase. Proc Natl Acad Sci U S A 108:19955–19960

Stevens TH, Forgac M (1997) Structure, function and regulation of the vacuolar H$^+$-ATPase. Annu Rev Cell Dev Biol 13:779–808

Tanigawara M, Tabata KV, Ito Y, Ito J, Watanabe R, Ueno H, et al. (2012) Role of the DELSEED Loop in Torque Transmission of F_1-ATPase. Biophys J 103:970–978

Usukura E, Suzuki T, Furuike S, Soga N, Saita E, Hisabori T, et al. (2012) Torque generation and utilization in motor enzyme F_0F_1-ATP synthase. Half-torque F_1 with short-sized pushrod helix and reduced ATP synthesis by half-torque F_0F_1. J Biol Chem 287:1884–1891

Yamamoto M, Unzai S, Saijo S, Ito K, Mizutani K, Sunolkeda C, et al. (2008) Interaction and stoichiometry of the peripheral stalk subunits NtpE and NtpF and the N-terminal hydrophilic domain of NtpI of *Enterococcus hirae* V-ATPase. J Biol Chem 283:19422–19431

Zhou M, Morgner N, Barrera NP, Politis A, Isaacson SC, Vinković DM, et al. (2011) Mass spectrometry of intact V-type ATPases reveals bound lipids and the effects of nucleotide binding. Science 334:380–385